Triangle comparison and space vector approaches to pulsewidth modulation in inverter-fed drives

G. Narayanan and V. T. Ranganathan*
Department of Electrical Engineering, Indian Institute of Science, Bangalore 560 012, India
Ph: 91-80-3600566; Fax: 91-80-3600444; email: vtran@ee.iisc.ernet.in

Abstract

This paper investigates the equivalence of the two popular approaches to pulsewidth modulation (PWM) in induction motor drives, namely, the triangle comparison approach and the space vector approach. It brings out the conditions wherein they are equivalent and wherein they are not. It shows that the space vector approach is more general and offers more degrees of freedom compared to the triangle comparison approach. Even a limited exploitation of these flexibilities has been reported to have improved the drive performance significantly. This gives adequate motivation to exploit these flexibilities further.

Keywords: Pulsewidth modulation, induction motor drives, inverters, space vector, variable speed drives and vectors.

1. Introduction

In real-time pulsewidth modulation (PWM) techniques[1–10] like the sine-triangle PWM[1] and the conventional space vector modulation,[2] a fundamental cycle is divided into several subcycles. The 3-phase voltages to be applied on the motor are specified in every subcycle and are met in an average sense. Thus, a volt–second balance is maintained over every subcycle.

There are two popular approaches to real-time PWM, namely, the triangle comparison approach and the space vector approach.

In the triangle comparison approach, 3-phase modulating waves are compared against a common triangular carrier to determine the switching instants of the three phases. The modulating wave of a given phase specifies the duty ratio or the average pole voltage corresponding to that phase. Switching the phase at an appropriate instant ensures that the required average pole voltage over the given half-carrier cycle is met. The most common and popular modulating waves are sinusoidal waves.[1] Any triplen frequency component can be added as the zero sequence component to the 3-phase sinusoidal waves. Different triplen frequency components thus lead to different modulating waves with different spectral properties. The choice of these triplen frequency components is a degree of freedom in this approach.[4–7]

A voltage source inverter is shown in Fig. 1. It has eight switching states. The voltage vectors corresponding to these eight states are as shown in Fig. 2. In the space vector approach, the voltage reference is provided in terms of a revolving space vector. The magnitude and the frequency of the fundamental component are specified by the magnitude and frequency, respec-
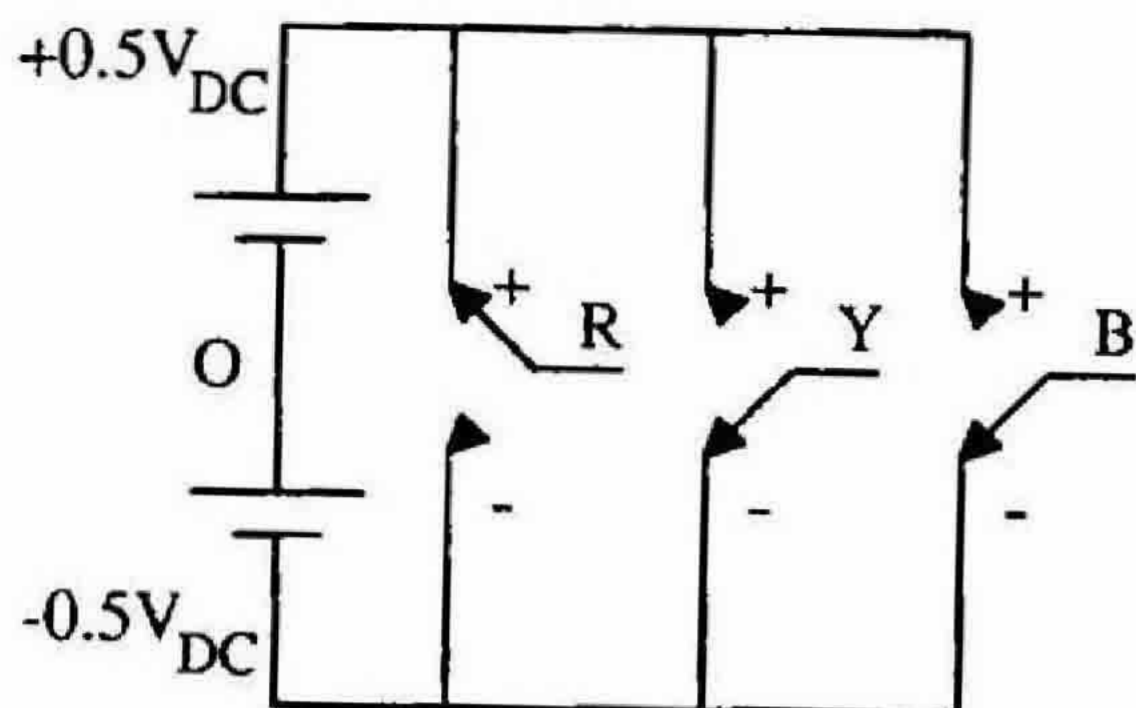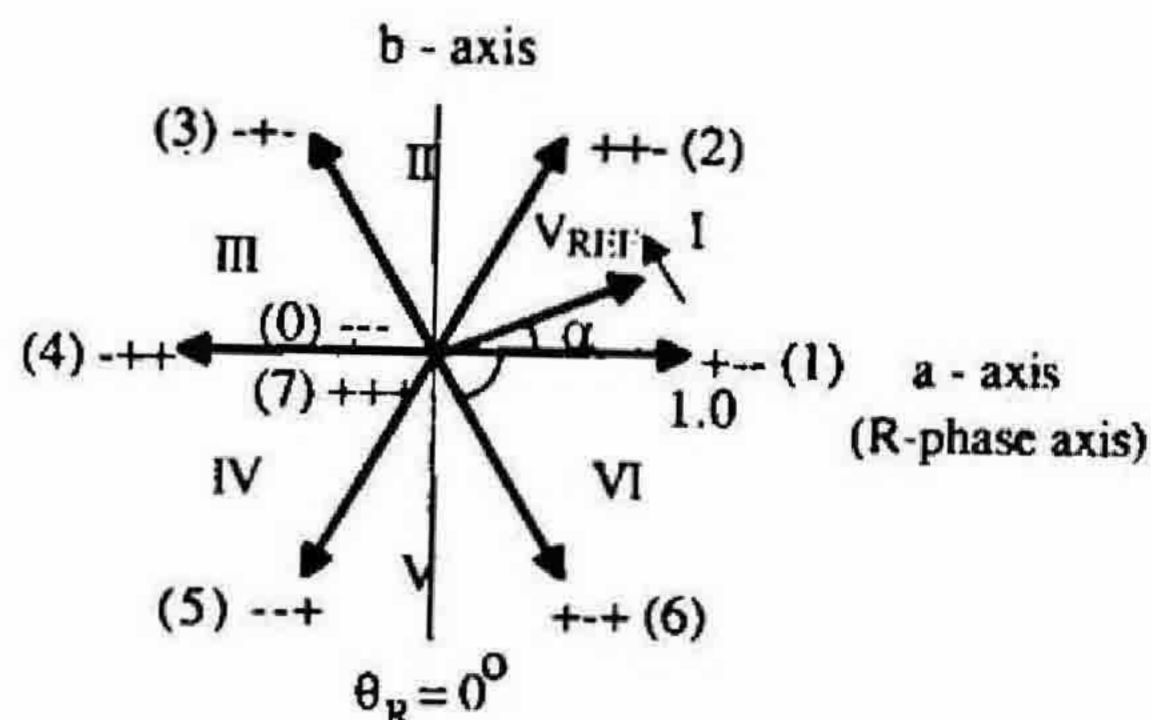
FIG. 1. Voltage source inverter.

FIG. 2. Voltage space vectors produced by an inverter. θ_R = angle of R-phase fundamental voltage. I, II, III, IV, V and VI: Sectors.

tively, of the reference vector. The reference vector is sampled once in every subcycle. The inverter is maintained in different states for appropriate durations such that an average voltage vector equal to the sampled reference vector is generated over the given subcycle. The inverter states used are the two zero states and the two active states whose voltage vectors are the closest to the commanded voltage vector. For a commanded vector in sector I, the states 0, 1, 2 and 7 can be used. To generate this vector in an average sense, the durations for which the active state 1, the active state 2, and the two zero states together must be applied are given by T_1, T_2 and T_Z, respectively, in eqn (1).

$$T_1 = T_S * V_{REF} \sin(60°-\alpha)/\sin(60°), \quad T_2 = T_S * V_{REF} \sin(\alpha)/\sin(60°), \quad T_Z = T_S - T_1 - T_2. \quad (1)$$

The division of the duration T_Z between the two zero states 0 and 7 is a degree of freedom in the space vector approach. This division of T_Z in a subcycle is equivalent to adding a common-mode component to the 3-phase average pole voltages. Over a fundamental cycle, this is equivalent to the addition of triplen frequency components to the fundamental sinusoidal waves in the triangle comparison approach.[4–6] That is, the same PWM waveform can be generated based on both the approaches. Hence, it has been concluded in the literature[4–6] that the two approaches are equivalent. This equivalence has been exploited to make the implementation easier, both when the voltage reference is available as 3-phase sinusoidal modulating waves[7] or as a voltage space vector.[8]

This paper investigates the equivalence of the two approaches in greater detail and in the light of newer PWM techniques reported.[9, 10] That is, it studies whether the same PWM waveforms, generated based on the space vector approach, can be generated using the triangle comparison approach as well. It brings out the conditions wherein such an equivalence does not exist and establishes that the space vector approach is more general than the triangle comparison approach.

2. Analysis at a subcycle level

Several space-vector-based PWM techniques have been reported.[2, 3, 8–12] It is to be studied whether the PWM waveforms generated by every one of these techniques can be generated using the triangle comparison approach as well. A fundamental cycle is divided into several subcycles in real-time PWM, as mentioned earlier. Hence, the equivalence can first be studied at the subcycle level.

Different switching sequences can be used to generate a given average vector in the space vector approach. For the same average vector, different switching sequences result in different sets of switching instants of the three phases. It is studied whether the same switching instants can be determined based on the triangle comparison approach as well.

2.1. Switching sequences

Given an average vector in sector I, the states that can be used are 0, 1, 2 and 7. Both the zero states can be used to generate the given average vector using sequences 0127 or 7210. These are termed as Type-I sequences here. The total zero state duration is divided equally between the two zero-states in the conventional space vector modulation, while it is divided unequally in modified space vector modulation.[11, 12] Alternatively, only one zero state can be used to generate the given average vector. Thus, sequences 012, 210, 721 or 127 can be used to generate the given average vector in sector I. These involve only two switchings instead of three. Such sequences are termed as Type-II sequences in this paper.

It can be seen that the active state 1 can as well be applied over more than one interval, all falling within the given subcycle and adding up to T_1, to generate the given average vector. This applies to the active state 2 as well. Hence, sequences like 0121, 1210, 7212 or 2127, where an active state time is divided into two equal halves, can also be used to generate the given average vector.[9-11] These sequences are termed as Type-III sequences here.

All the three types of sequences can be used to generate any arbitrary average vector. An arbitrary vector needs both the active vectors. However, an average vector along a sector boundary needs only one active vector. For a vector on the boundary between sectors VI and I, the active vector 1 alone is needed. Hence, sequence 010 or 101 can be used to generate such an average vector.[9, 10] These are termed as Type-IV sequences here.

2.1.1. Type-I sequences

The pole voltages and the line voltages, normalized with respect to $0.5V_{DC}$, over the given subcycle are as shown in Figs 3a and b for sequences 0127 and 7210, respectively. All the three phases switch once within the subcycle. The duty ratios of the three phases in the given subcycle depend on V_{REF} and α as shown below :

$$d_R = (T_1 + T_2 + T_7)/T_S = 0.5 + 0.5*V_{REF}*\cos(30°-\alpha)/\sin(60°),$$

$$d_Y = (T_2 + T_7)/T_S = 0.5 + V_{REF}*\sin(\alpha-30°),$$

$$d_B = T_7/T_S = 0.5 - 0.5*V_{REF}*\cos(30°-\alpha)/\sin(60°). \tag{2}$$

The average values of the 3-phase pole voltages over the given subcycle are also shown in dashed lines in Fig. 3 along with the respective pole voltages. The expressions for the average pole voltages, normalized with respect to $0.5V_{DC}$, for the three phases are :

$$m_R = 2(d_R-0.5) = V_{REF}*\cos(30°-\alpha)/\sin(60°),$$

$$m_Y = 2(d_Y-0.5) = 2*V_{REF}*\sin(\alpha - 30°),$$

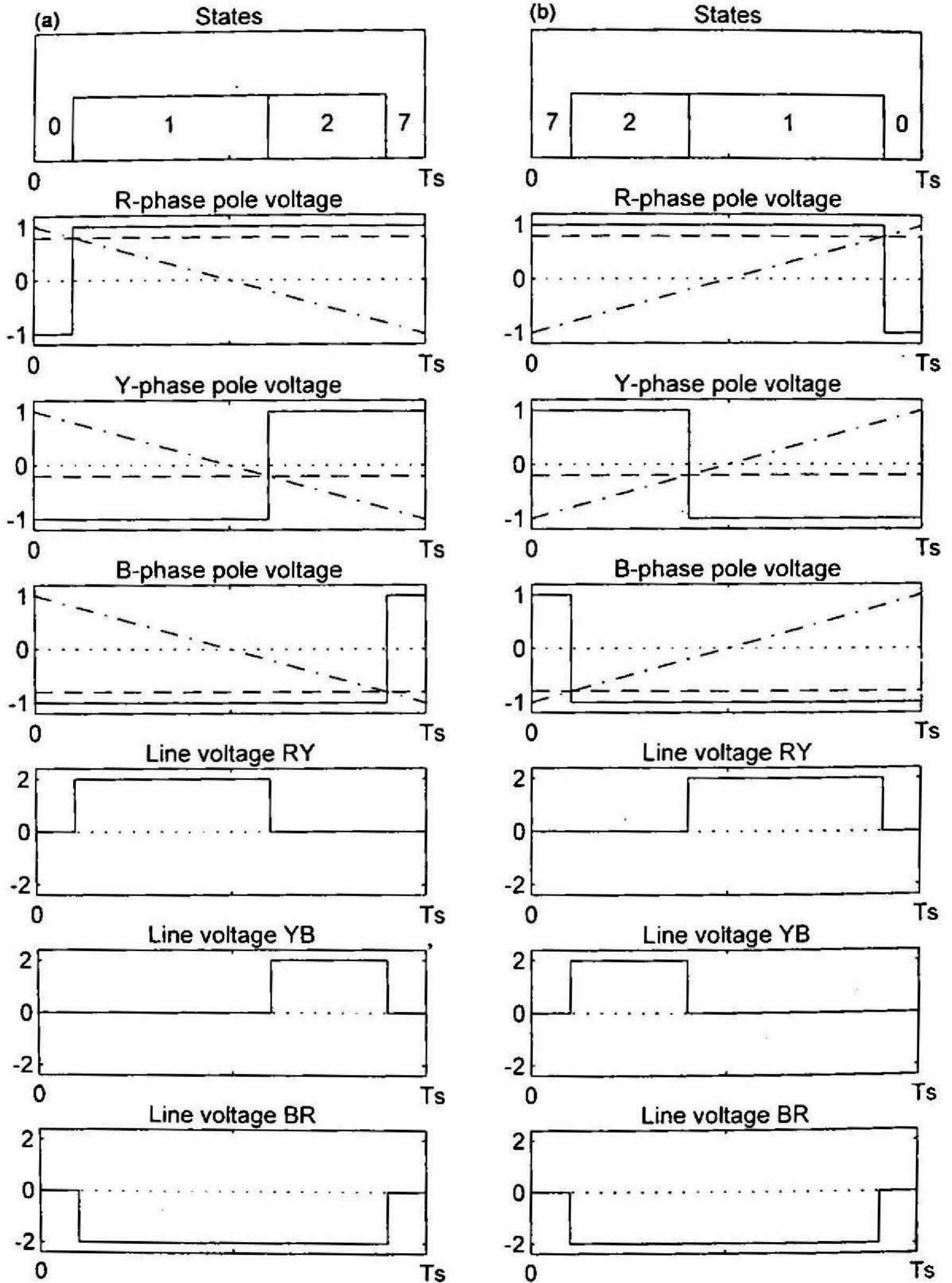$$m_B = 2(d_B-0.5) = -V_{REF}*\cos(30°- \alpha)/\sin(60°). \tag{3}$$

FIG. 3. Transitions in a subcycle: Sequences (a) 0127 and (b) 7210.

It can be seen that the sum of the three average pole voltages is not zero, implying the presence of a common-mode component. The mean value of these three average pole voltages is the common-mode component. Average pole voltage minus the common-mode component is the component that actually drives the motor currents. This component is termed here as the sinusoidal component of the average pole voltage.

The common-mode component over the given subcycle is :

$$m_C = (m_R + m_Y + m_B)/3 = 2*V_{REF}*\sin(\alpha - 30°)/3. \tag{4}$$

The sinusoidal components of the 3-phase average pole voltages over the given subcycle are :

$$m_{SR} = V_{REF}*\cos(30° - \alpha)/\sin(60°) - 2*V_{REF}*\sin(\alpha - 30°)/3,$$
$$m_{SY} = 4*V_{REF}*\sin(\alpha - 30°)/3,$$
$$m_{SB} = -V_{REF}*\cos(30 - \alpha)/\sin(60°) - 2*V_{REF}*\sin(\alpha - 30°)/3. \tag{5}$$

Thus,

$$m_C = 0.5*m_{SY}. \tag{6}$$

Thus, when a Type-I sequence is used to generate the given average vector, the common-mode component is half the sinusoidal component of the phase that switches between the two active states in the given sector.

Comparing the average pole voltages with a falling ramp as shown in Fig. 3a gives the same switching instants of the individual phases as with the sequence 0127. In the case of sequence 7210, the ramp is a rising one as shown in Fig. 3b. Thus, when Type-I sequences are used, the same switching instants can be determined using the triangle comparison approach as well. In other words, Type-I sequences have equivalence in the triangle comparison approach.

2.1.2. Type-II sequences

Sequences 012, 210, 721 and 127 can be used for generating a sample in sector I. The switching states, pole and line voltages over a subcycle are shown in Fig. 4 for sequences 012 and 210, and in Fig. 5 for sequences 721 and 127.

Sequences 012 and 210

When a Type-II sequence using the zero state 0, namely 012 or 210, is used for generating an arbitrary average vector in sector I, the duty ratios of the three phases in the given subcycle are as follows :

$$d_R = (T_1 + T_2)/T_S = V_{REF}*\cos(30° - \alpha)/\sin(60°),$$
$$d_Y = T_2/T_S = V_{REF}*\sin(\alpha)/\sin(60°),$$
$$d_B = 0. \tag{7}$$

The average pole voltages, normalized with respect to $0.5V_{DC}$, of the three phases over the given subcycle are as follows:

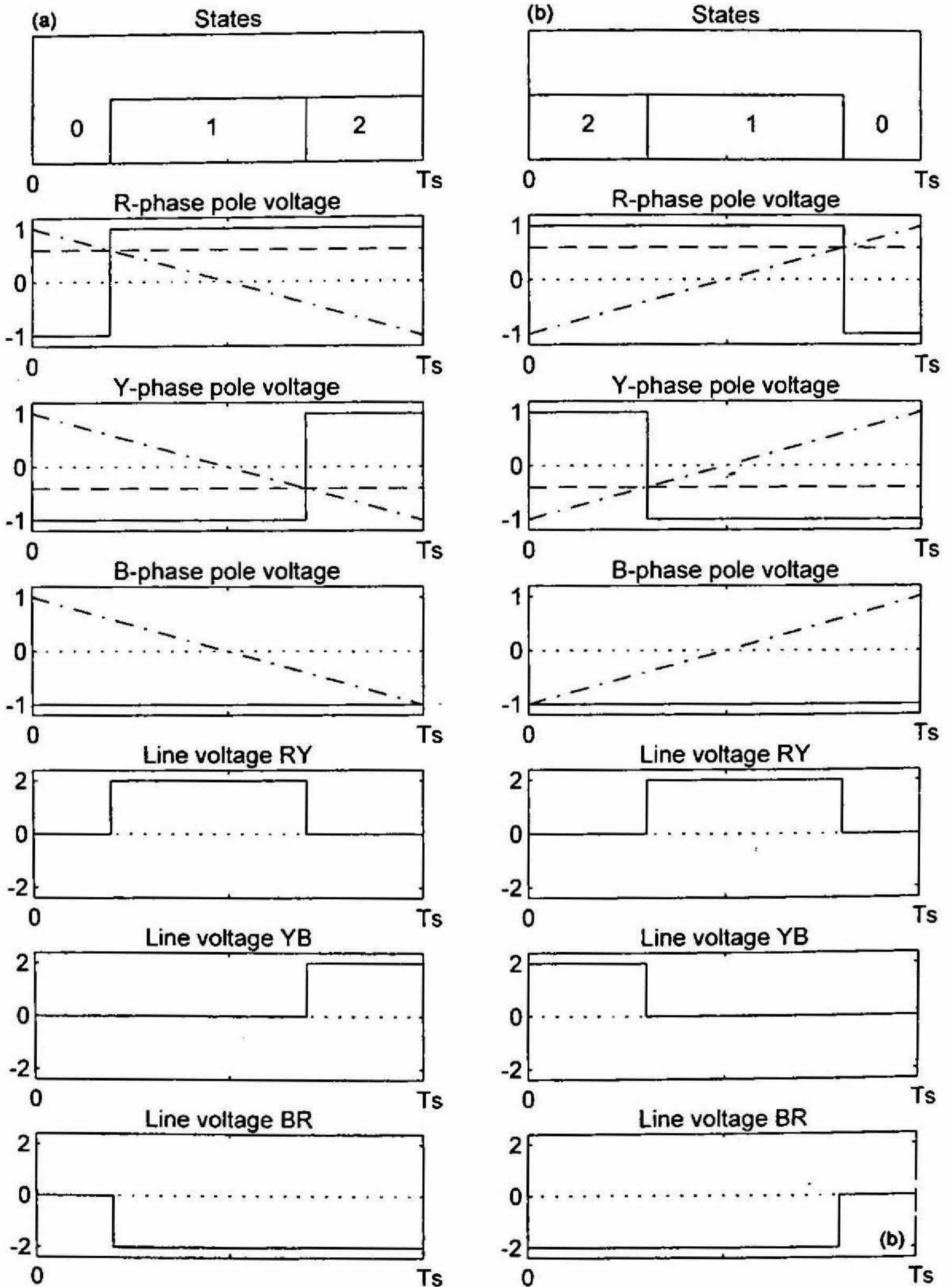$$m_R = 2(d_R - 0.5) = 2*V_{REF}*\cos(30° - \alpha)/\sin(60°) - 1,$$

FIG. 4. Transitions in a subcycle: Sequences (a) 012 and (b) 210.

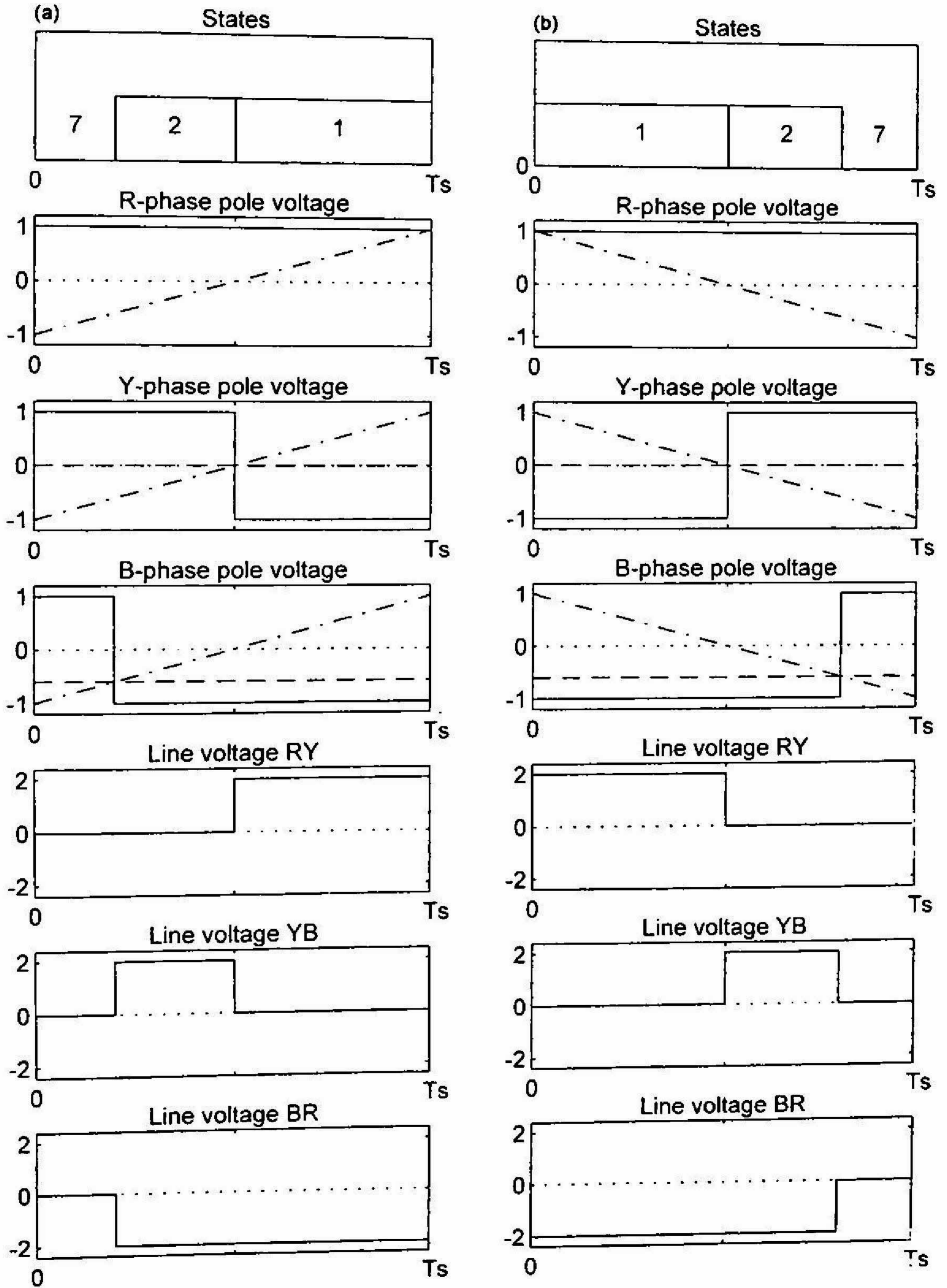FIG. 5. Transitions in a subcycle: Sequences (a) 721 and (b) 127.

$$m_Y = 2(d_Y - 0.5) = 2*V_{REF}*\sin(\alpha)/\sin(60°) - 1,$$

$$m_B = 2(d_B - 0.5) = -1. \tag{8}$$

The common-mode component and the sinusoidal components of the three phases are as follows :

$$m_C = (m_R + m_Y + m_B)/3 =$$
$$(2/3)*V_{REF}*\cos(30° - \alpha)/\sin(60°) + (2/3)*V_{REF}*\sin(\alpha)/\sin(60°) - 1, \tag{9}$$

$$m_{SR} = (4/3)*V_{REF}*\cos(30° - \alpha)/\sin(60°) - (2/3)*V_{REF}*\sin(\alpha)/\sin(60°),$$

$$m_{SY} = -(2/3)*V_{REF}*\cos(30° - \alpha)/\sin(60°) + (4/3)*V_{REF}*\sin(\alpha)/\sin(60°),$$

$$m_{SB} = -(2/3)*V_{REF}*\cos(30° - \alpha)/\sin(60°) - (2/3)*V_{REF}*\sin(\alpha - 30°)/\sin(60°). \tag{10}$$

Hence,

$$m_C = -1 - m_{SB}. \tag{11}$$

Thus, the common-mode component is related to the sinusoidal component of the phase which is clamped during the given subcycle, and can be derived from this component.

(b) Sequences 721 and 127

When a Type-II sequence using the zero state 7, namely 721 or 127, is used for generating an arbitrary average vector in sector I, the duty ratios of the three phases in the given subcycle are as follows :

$$d_R = 1,$$
$$d_Y = (T_7 + T_2)/T_S = 1 - V_{REF}*\sin(60° - \alpha)/\sin(60°),$$
$$d_B = T_7/T_S = 1 - V_{REF}*\cos(30° - \alpha)/\sin(60°). \tag{12}$$

The average pole voltages, normalized with respect to $0.5V_{DC}$, and the common-mode component of the average pole voltages are as follows :

$$m_R = 2(d_R - 0.5) = 1,$$
$$m_Y = 2(d_Y - 0.5) = 1 - 2*V_{REF}*\sin(60° - \alpha)/\sin(60°),$$
$$m_B = 2(d_B - 0.5) = 1 - 2*V_{REF}*\cos(30° - \alpha)/\sin(60°), \tag{13}$$
$$m_C = (m_R + m_Y + m_B)/3$$
$$= 1 - (2/3)*V_{REF}*\sin(60° - \alpha)/\sin(60°) - (2/3)*V_{REF}*\cos(30° - \alpha)/\sin(60°). \tag{14}$$

The sinusoidal components of the average pole voltages of the three phases are :

$$m_{SR} = (2/3)*V_{REF}*\sin(60° - \alpha)/\sin(60°) + (2/3)*V_{REF}*\cos(30° - \alpha)/\sin(60°),$$

$$m_{SY} = -(4/3)*V_{REF}*\sin(60° - \alpha)/\sin(60°) + (2/3)*V_{REF}*\cos(30° - \alpha)/\sin(60°),$$

$$m_{SB} = (2/3)*V_{REF}*\sin(60° - \alpha)/\sin(60°) - (4/3)*V_{REF}*\cos(30° - \alpha)/\sin(60°). \tag{15}$$

Hence,

$$m_C = 1 - m_{SR}. \tag{16}$$

Thus, the common-mode component is related to the sinusoidal component of the phase, which is clamped during the given subcycle as earlier.

The average pole voltages for the three phases over the given subcycle are shown in Figs.4 and 5. Comparing these average pole voltages with ramps as shown in the figures gives the switching instants of the individual phases. The ramps are falling ones in case of sequences 012 and 127, while they are rising ones in case of sequences 721 and 210. Thus, Type-II sequences also have equivalence in the triangle comparison approach.

2.1.3. Type-III sequences

Switching sequences 0121, 1210, 7212 or 2127 can also be used to generate an arbitrary average vector in sector I. The switching states, pole voltages and line voltages over a subcycle are shown for all these four sequences in Figs 6 and 7.

The duty ratios and the average pole voltages of three phases in the case of sequences 0121 and 1210 are identical to those in the case of sequences 012 and 210. Similarly, the duty ratios and the average pole voltages in the case of 7212 and 2127 are identical to those in the case of 721 and 127. Hence, the expressions given in Section 2.1.2 are valid for Type-III sequences as well.

The average pole voltages of the three phases over the given subcycle while generating the given commanded vector are shown in Figs 6 and 7. The Y-phase switches twice within the subcycle. Hence, the switching instants of this phase cannot be determined by comparing its average pole voltage with a ramp as in the earlier cases. Thus, there is no equivalence for Type-III sequences in the triangle comparison approach.

If the switching instants of the Y-phase are to be determined using its average pole voltage, then the signal used for comparison must be an asymmetric double ramp (instead of a ramp) as shown in dashed and dotted lines in Figs 6 and 7. The two ramps, which constitute this signal, have different slopes. They divide the subcycle into two unequal durations, namely T_a and T_b, as shown. Their relative slopes change with change in the average pole voltage. The average pole voltage varies with both V_{REF} and α. Thus, the signal required for comparison is dependent on both V_{REF} and α.

In addition, the asymmetric double-ramp signal cannot be used for the other phase that switches. For this phase, the comparison of the average pole voltage must be done with a ramp as in the case of Type-I and II sequences. Thus, the signals to be used for comparison are different for different phases.

The implications of the above are that the three phases cannot have a common carrier and the carrier waveshape itself is dependent on the modulation index.

2.1.4. Type-IV sequences

Switching sequences 010 and 101 can be used to generate an average vector on the boundary between sectors VI and I. The states, pole and line voltages within the subcycle are shown in Fig. 8. The duty ratios and the average pole voltages of the three phases over the subcycle are as shown below :

$$d_R = V_{REF},$$
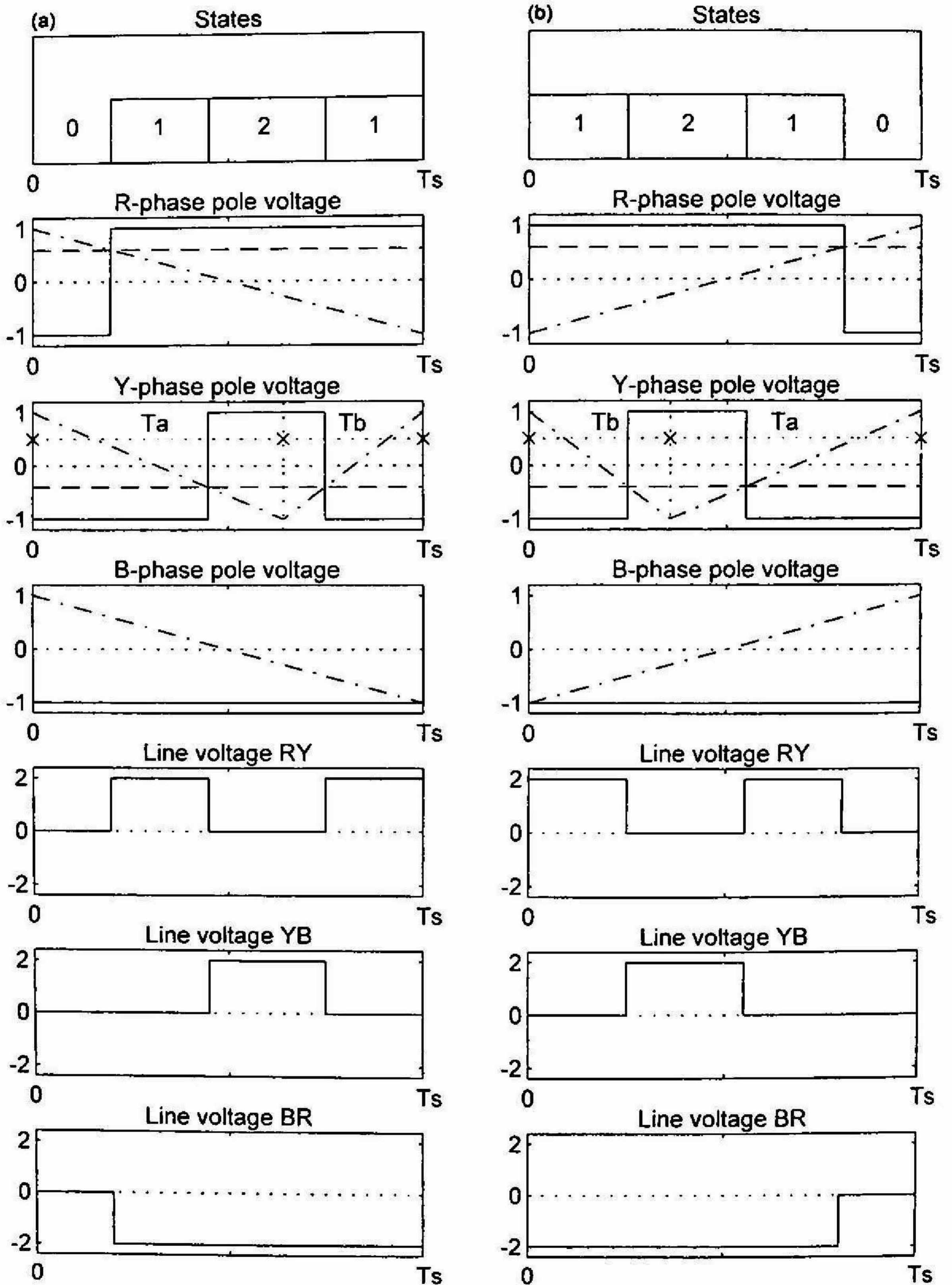$$d_Y = 0,$$
$$d_B = 0. \tag{17}$$

FIG. 6. Transitions in a subcycle: Sequences (a) 0121 and (b) 1210.
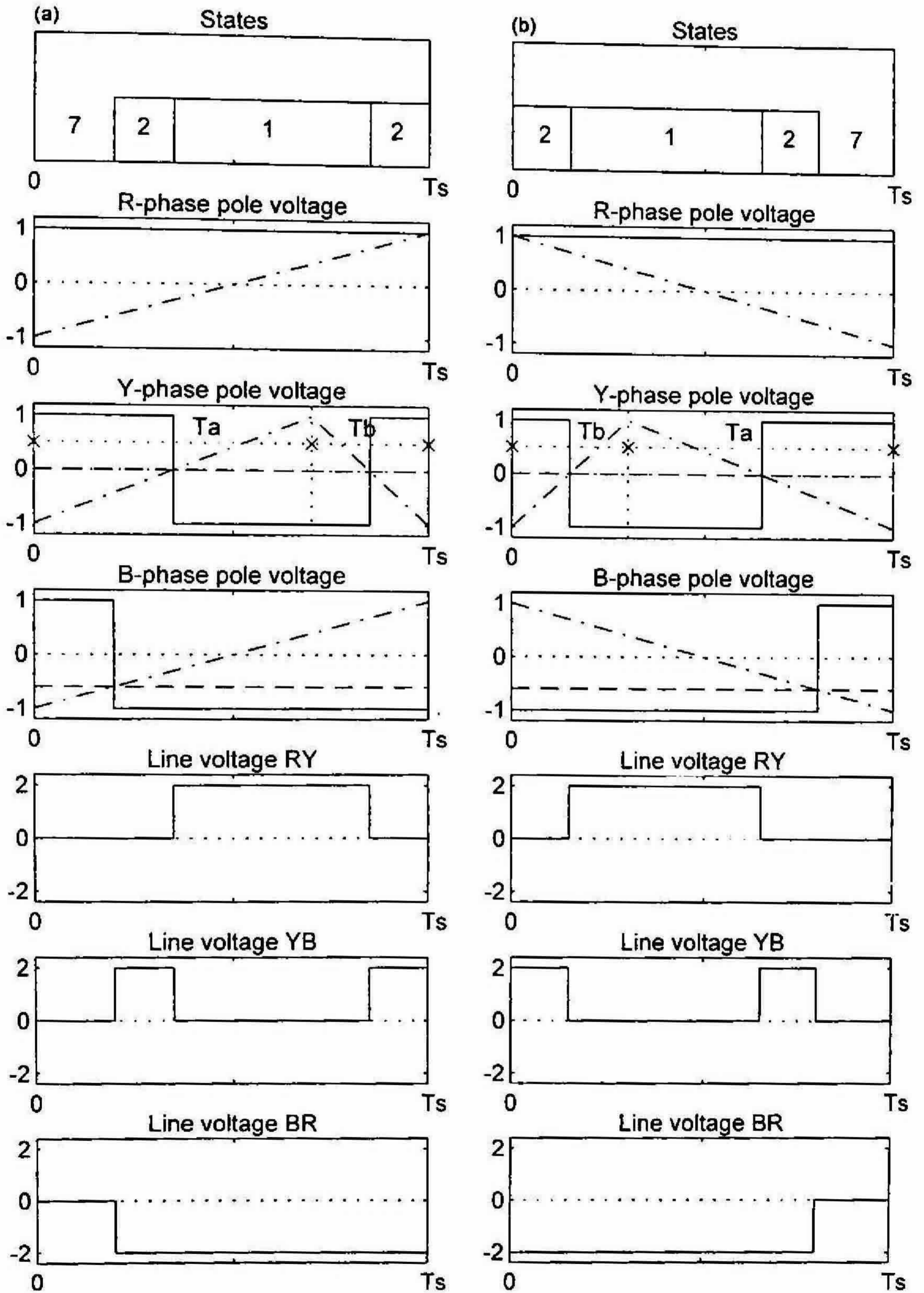
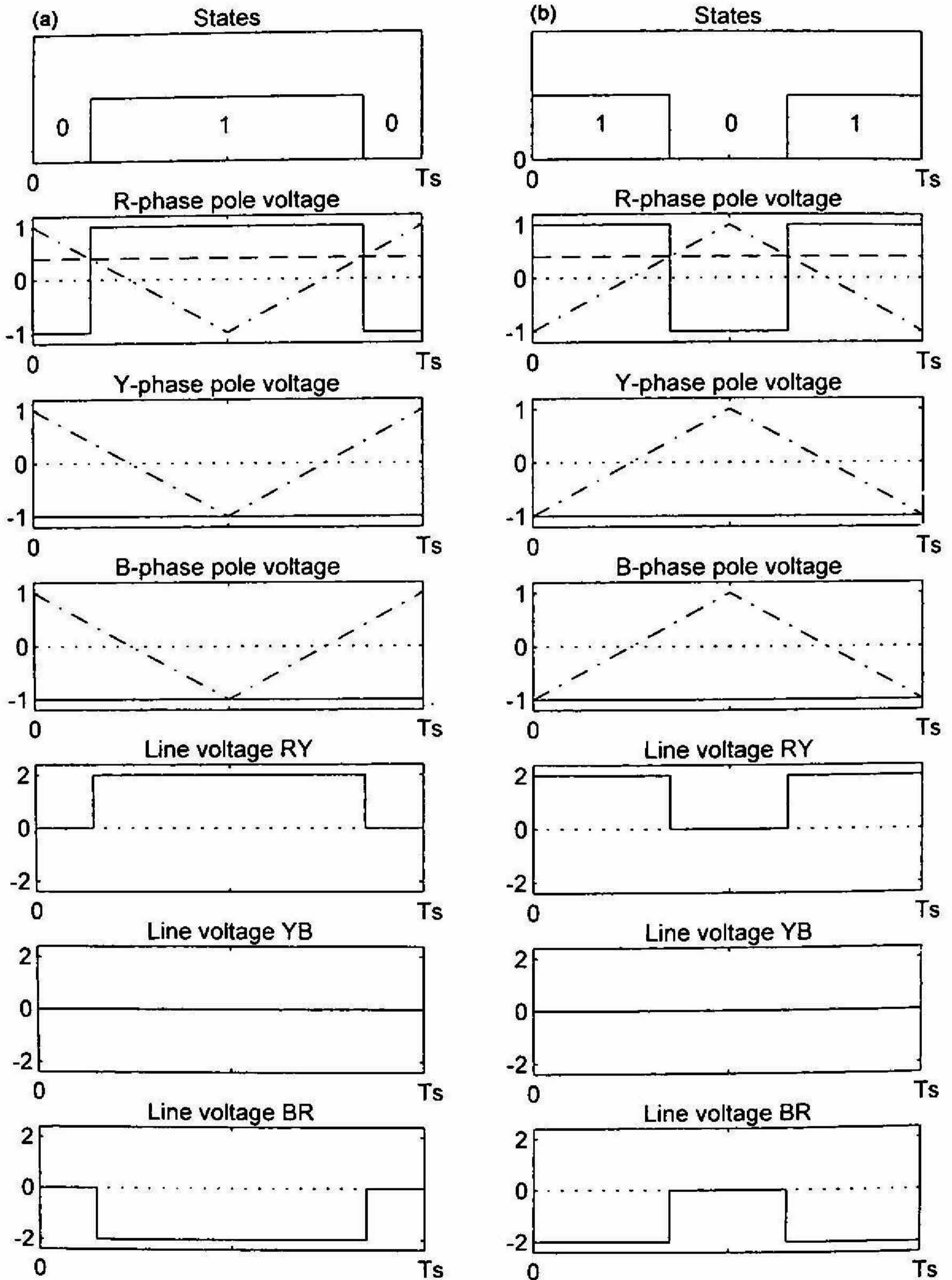FIG. 7. Transitions in a subcycle: Sequences (a) 7212 and (b) 2127.

FIG. 8. Transitions in a subcycle: Sequences (a) 010 and (b) 101.

$$m_R = 2(d_R - 0.5) = 2*V_{REF} - 1,$$
$$m_Y = 2(d_Y - 0.5) = -1,$$
$$m_B = 2(d_B - 0.5) = -1. \tag{18}$$

The average common-mode component is as shown below :

$$m_C = (m_R + m_Y + m_B)/3 = (2/3)*V_{REF} - 1. \tag{19}$$

The sinusoidal components of the 3-phase average pole voltages are:

$$m_{SR} = (4/3)*V_{REF}$$
$$m_{SY} = -(2/3)*V_{REF}$$
$$m_{SB} = -(2/3)*V_{REF}. \tag{20}$$

Hence,

$$m_C = -1 - m_{SY} = -1 - m_{SB} \tag{21}$$

Thus, the common-mode component is related to the sinusoidal components of the two phases that are clamped over the subcycle.

One phase switches twice, while the other two remain clamped over the given subcycle. The switching instants of the double-switching phase cannot be determined by comparing its average pole voltage with a ramp signal. Thus, there is no equivalence in the triangle comparison approach for Type-IV sequences also, as is the case with Type-III sequences.

If the switching instants of the double-switching phase are to be determined using its average pole voltage, then its average pole voltage must be compared against a double-ramp signal (instead of a ramp), as shown in Fig. 8. This signal is symmetric unlike the one in the case of Type-III sequences. Also, the shape of this signal does not vary with modulation index. Hence, the carrier waveshape is independent of the modulation index. This same signal can be used for the other two phases also. Hence, the three phases can have a common carrier.

The study was carried out at a subcycle level in this section. It will be done at a fundamental cycle level in the following section using some PWM strategies as example cases.

3. Equivalent modulating and carrier waves

Some space-vector-based synchronized PWM strategies have been reported recently.[9-10] Of these strategies, the conventional space vector strategy (CSVS) uses only the Type-I sequences, the basic bus clamping strategy (BBCS) uses Type-I and II sequences, the asymmetric zero-changing strategy (AZCS) uses Type-II and III sequences, and the boundary sampling strategy (BSS) uses Type-I, II and IV sequences.

The modulation process involved in any space-vector-based technique can be seen in terms of equivalent modulating and carrier waves, the comparison of which results in the same PWM waveforms as generated by the given technique. The equivalent modulating and carrier waves corresponding to these strategies are presented in this section. It is shown that the equivalent carrier waves are triangular waves only in the case of CSVS and BBCS. In the case of AZCS and BSS, which use Type-III and IV sequences, respectively, the
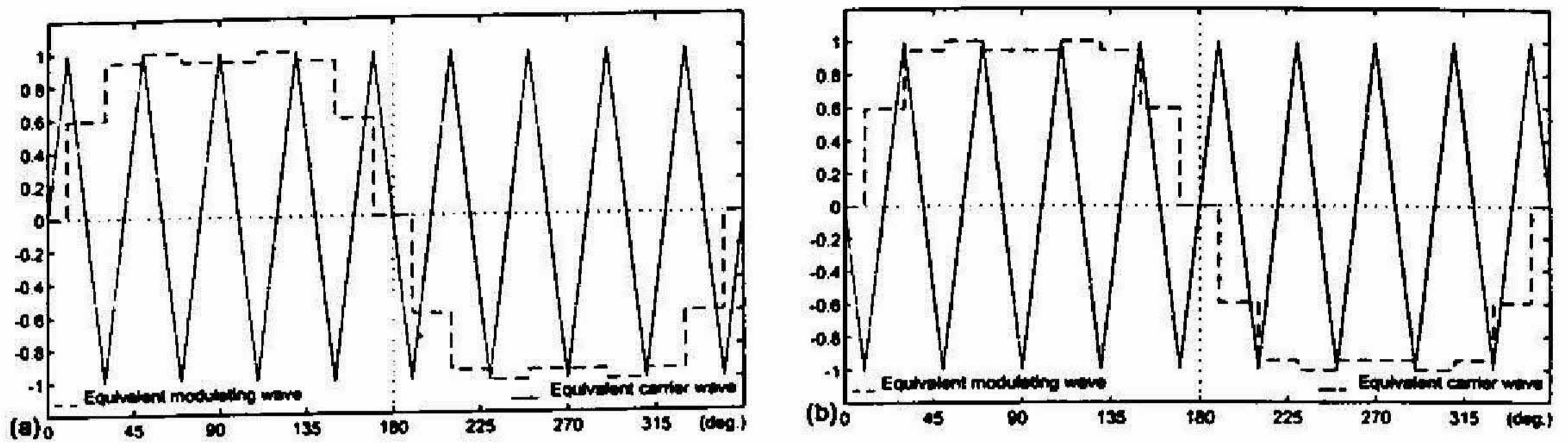
FIG. 9. Equivalent modulating and carrier waves – CSVS. (a) $N=3$, $V_{REF}=0.866$, case (i). (b) $N=3$, $V_{REF}=0.866$, case (ii).

equivalent carrier is not a regular, isosceles triangular wave. Instead it is irregular and/or discontinuous.

3.1. *Conventional space vector strategy (CSVS)*

The modulating wave in the triangle comparison approach is nothing but variation of the average pole voltage over a fundamental cycle. The variation of the average pole voltage and its two components over a fundamental cycle in the case of the conventional space vector strategy can be determined based on the expressions derived in Section 2.1.1. These average pole voltage waveforms are the equivalent modulating waves, which change with the modulation index.

In conventional space vector strategy with number of samples per sector $N = 3$,[9, 10] the sequences used during the three subcycles in sector I are **0127**, **7210** and **0127**, respectively. Alternatively, sequences **7210**, **0127** and **7210**, respectively, can also be used for the three samples. The former can be referred to as case (i), while the latter can be referred to as case (ii).

The average pole voltage for a given V_{REF} is the same for both the cases. This waveform corresponding to $V_{REF} = 0.866$ is shown in both Figs 9a and b in dashed lines. PWM patterns, identical to the ones produced by case (i), can be generated by comparing the average pole voltage wave with a triangular carrier wave, as shown in Fig. 9a. This carrier has a positive zero-crossing at the positive zero-crossing of the modulating sinusoidal component. Comparison of the same average pole voltage waveform with a triangular carrier as shown in Fig. 9b leads to PWM waveforms identical to the ones that can be generated by case (ii). This carrier wave has a negative zero-crossing at the positive zero-crossing of the modulating sinusoidal component, which is the preferred case in synchronized sine-triangle PWM.

3.2. *Basic bus clamping strategy (BBCS)*

Based on the expressions derived in Sections 2.1.1 and 2.1.2, the average pole voltage and its two components corresponding to BBCS can be calculated. The variation of the average pole voltage of a phase over a fundamental cycle corresponding to BBCS with $N = 5$[9, 10] is shown in Fig. 10 for $V_{REF} = 0.866$. Depending on the choice of the switching sequences used, BBCS with $N = 5$ produces two types of PWM waveforms, namely, 60° and 30° clamping waveforms. In the former, every phase is clamped during the middle 60° duration of every half cycle of its fundamental voltage. In the latter, every phase remains clamped during the middle
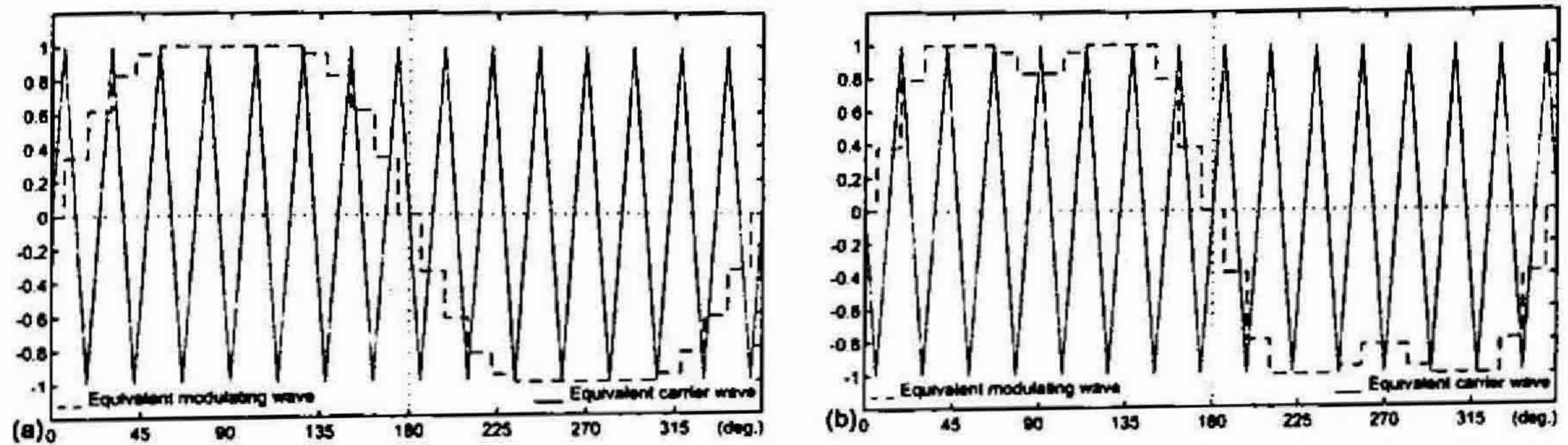
FIG. 10. Equivalent modulating and carrier waves – BBCS. (a) $N = 5$, 60° clamping, $V_{REF} = 0.866$ and (b) $N = 5$, 30° clamping, $V_{REF} = 0.866$.

30° duration of every quarter cycle of its fundamental voltage.[9–10] The variations of the average pole voltage corresponding to 60° and 30° clampings are shown in Figs 10a and 10b, respectively. These average pole voltage waveforms are the equivalent modulating waves corresponding to the different cases considered.

The equivalent carrier waves can be constructed using the ramp signals, discussed in Sections 2.1.1 and 2.1.2. The equivalent carrier waves are triangular carrier waves once again as in the case of the conventional space vector strategy, and are shown in Fig. 10.

In the case of 60° clamping, the carrier wave has a positive zero-crossing at the positive zero-crossing of the modulating sinusoidal component as in case (i) of the conventional space vector strategy. It may be noted that the sequence used for the middle sample of sector I is **7210** in both these cases.

In the case of 30° clamping, the carrier wave has a negative zero-crossing at the positive zero-crossing of the modulating sinusoidal component as in case (ii) of the conventional space vector strategy. It may be noted that the sequence used for the middle sample of sector I is **0127** in both these cases.

Thus, the PWM patterns, identical to the ones generated by BBCS, can be generated by comparing these equivalent modulating and carrier waves. The nature of the common-mode components is different for the conventional space vector strategy and BBCS with 60° and 30° clampings. The equivalent carrier waves are regular, isosceles triangular waves for both these strategies, which are the synchronized versions of the conventional and the modified forms of
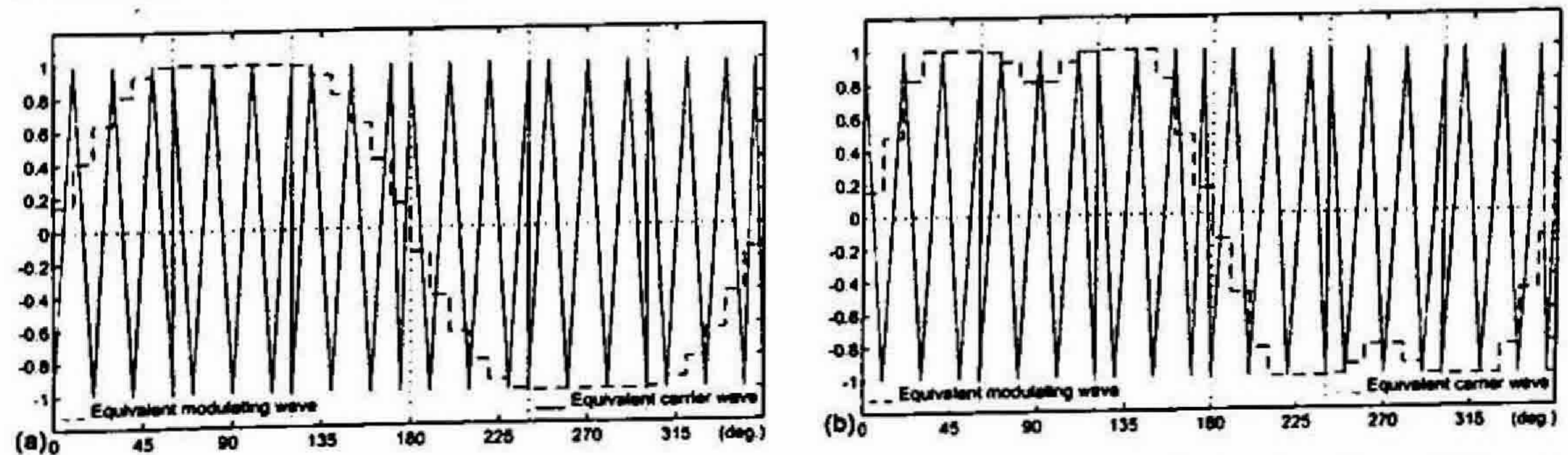

FIG. 11. Equivalent modulating and carrier waves of one phase – AZCS. (a) $N = 6$, 60° clamping, $V_{REF} = 0.866$ and (b) $N = 6$, 30° clamping, $V_{REF} = 0.866$.

space vector modulation, discussed in the literature.[11, 12] Such a study is carried out in the following sections for two other synchronised PWM strategies.

3.3. Asymmetric zero-changing strategy (AZCS)

The equivalent modulating and carrier waves corresponding to AZCS with $N = 6$ and $60°$ clamping[9, 10] and $N = 6$ and $30°$ clamping[9, 10] are shown in Fig. 11 a and b, respectively, both for $V_{REF} = 0.866$. It can be seen that the equivalent carrier waves are discontinuous at $60°$, $120°$, $240°$ and $300°$. The asymmetric double ramp can be seen in the subcycles ending with $180°$ and $360°$. Thus, the equivalent carrier waves are irregular and have a periodicity equal to the fundamental period.

The equivalent carrier waves corresponding to AZCS with $N = 6$ and $30°$ clamping scheme for the same V_{REF} are shown in Figs 12a, b and c for R-, Y- and B-phases respectively. It can be seen that the carrier waves are different for the three phases.

3.4. Boundary sampling strategy (BSS)

The average pole voltage waveforms corresponding to BSS with $N = 4$ and $N = 6$[9, 10] are presented in Figs 13a and b, respectively, for $V_{REF} = 0.866$. The corresponding equivalent carrier waves are also shown. The symmetric double ramp can be seen in the subcycles where Type IV sequences are used. In the case of $N = 4$, the carrier is discontinuous at the start and end of such subcycles. The periodicity of the equivalent carrier waves is one third of the fundamental period.
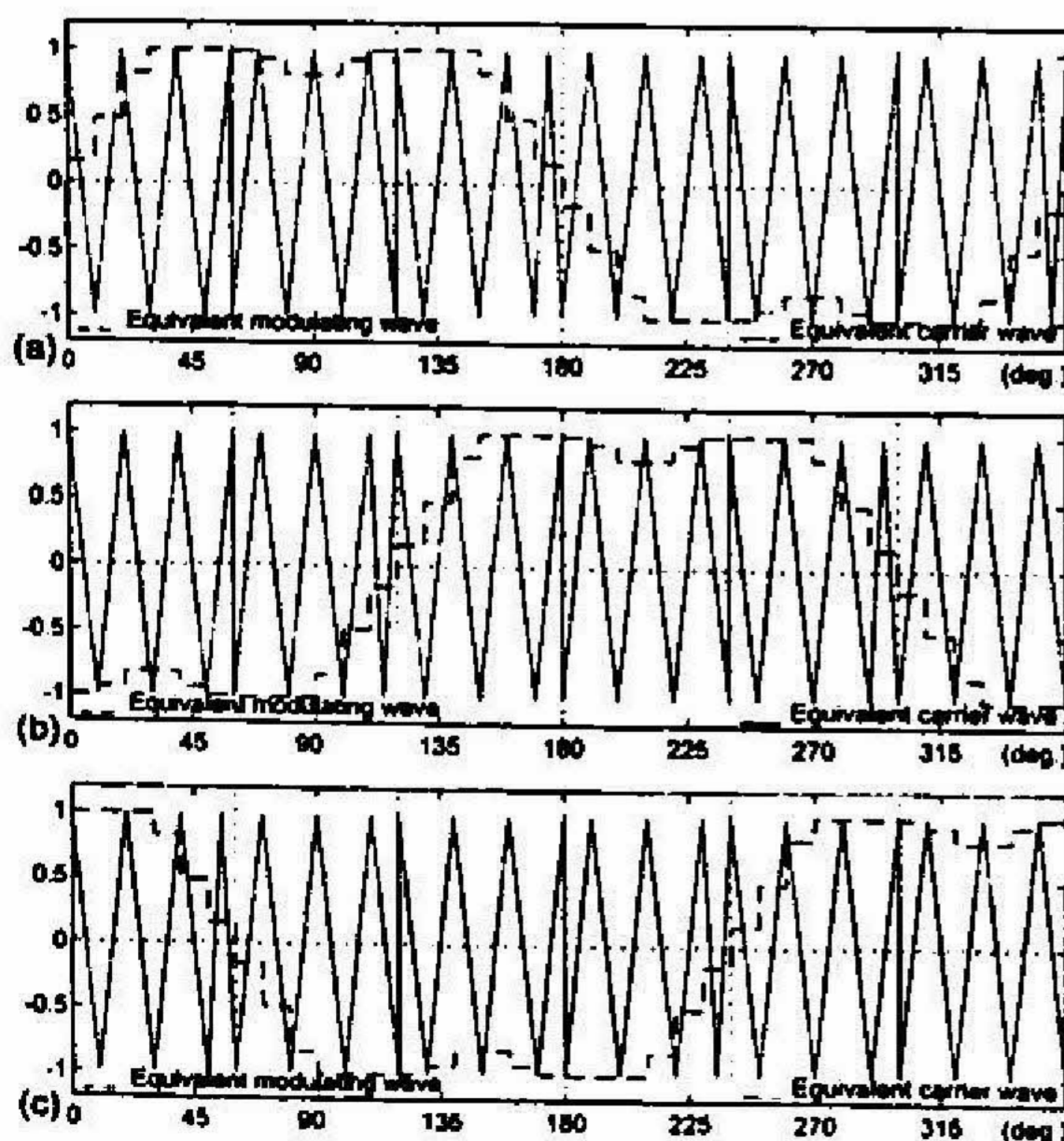

FIG. 12. Equivalent modulating and carrier waves of 3 phases – AZCS. (a) R-phase, $N = 6$, $30°$ clamping, V_{REF} = 0.866, (b) Y-phase, $N = 6$, $30°$ clamping, V_{REF} = 0.866 and (c) B-phase, $N = 6$, $30°$, clamping, V_{REF} = 0.866.
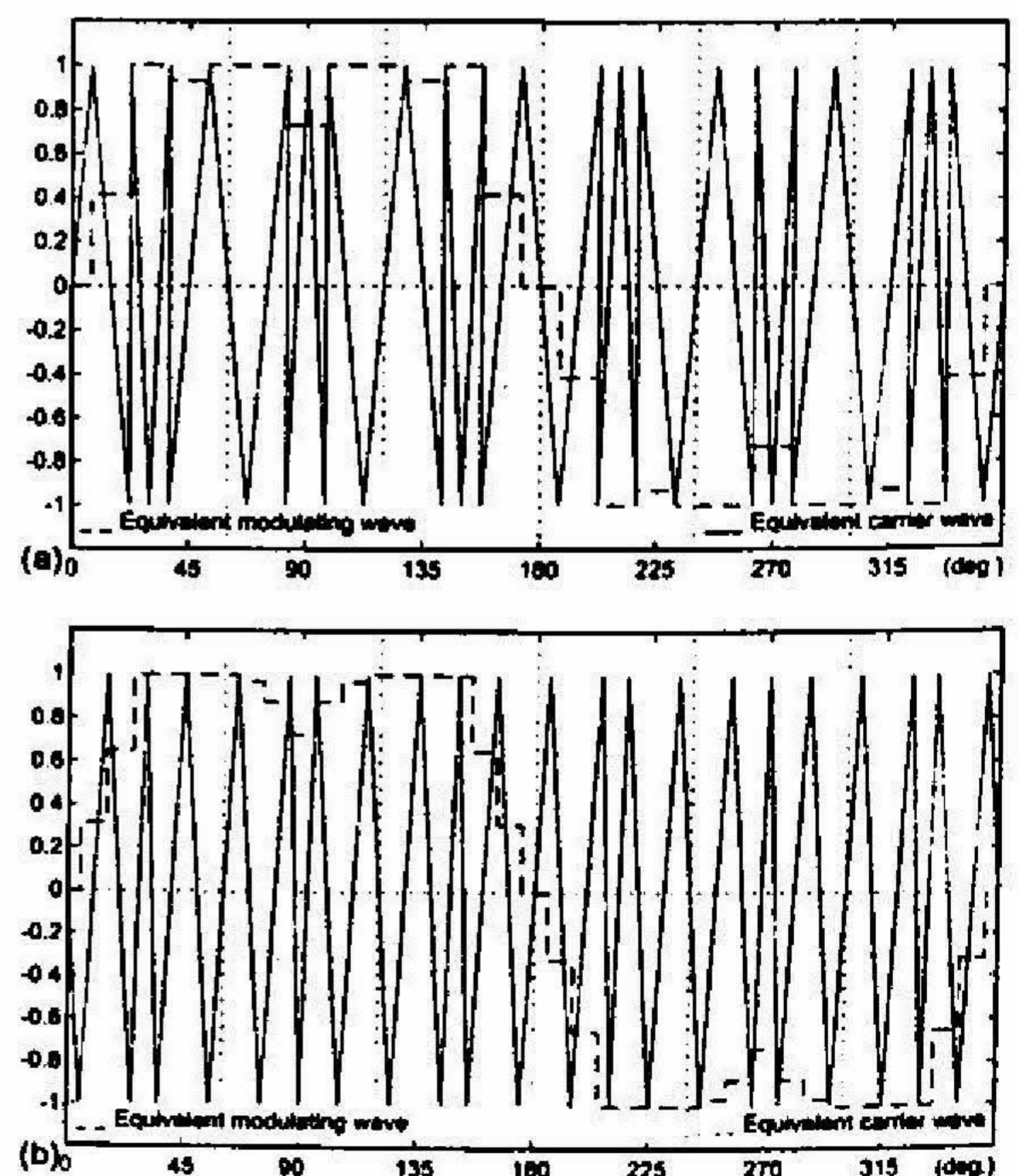

FIG. 13. Equivalent modulating and carrier waves – BSS. (a) $N = 4$, V_{REF} = 0.866 and (b) $N = 6$, V_{REF} = 0.866.

In the triangle comparison approach, the number of half-carrier cycles per 180° must be odd for half-wave symmetry and even per 120° for 3-phase symmetry. Hence, the number of half-carrier cycles per 60° must be odd. On the other hand, the number of subcycles per sector can either be odd or even in the space vector approach.

3.5. Performance

The total harmonic distortion factor of the no-load current waveform (I_{THD}), or equivalently, the weighted total harmonic distortion factor of the line voltage waveform (V_{WTHD}) is a suitable performance measure for evaluating different PWM strategies.

$$I_{THD} = \frac{\sqrt{\sum I_n^2}}{I_1}, n \neq 1 \tag{22}$$

$$V_{WTHD} = \frac{\sqrt{\sum (V_n / n)^2}}{V_1}, n \neq 1 \tag{23}$$

where I_1 and I_n are the RMS values of the fundamental and the nth harmonic currents, respectively, and V_1 and V_n are the RMS values of the fundamental and the nth harmonic voltages, respectively.

The use of Type-III sequences leads to lesser current ripple at higher modulation indices over Type-I sequences.[11] For a pulse number of 9, the computed V_{WTHD} vs M characteristics are presented for CSVS, AZCS and BSS in Fig. 14a. The corresponding measured I_{THD} vs M characteristics are presented in Fig. 14b. It can be seen that AZCS and BSS perform better than any other comparable strategy at different ranges of modulation indices. Thus, Type-III and IV sequences help in improving the performance of motor drives significantly at middle and higher speed ranges.

4. Discussion

In Fig. 3, the total zero-state duration T_Z is equally divided between the zero states 0 and 7. For the same T_Z if T_0 is decreased and T_7 increased, it can be seen that all the three average pole voltages increase and by the same measure. That is, it is only their common-mode component that changes, and not the sinusoidal components. The relation between the ratio of division of T_Z and the common-mode component has been brought out by Blasko.[4] Using this, the PWM waveforms generated by any triangle comparison-based PWM technique can be generated using the space-vector approach as well. Similarly, the PWM waveforms generated by any space-vector-based PWM technique, using Type-I and II sequences alone, can be generated based on the triangle comparison approach also. Thus, when only Type-I and II sequences are used, the space vector approach is equivalent to the triangle comparison approach.

This equivalence has found use in simplifying PWM calculations. From Figs 4 to 6 it can be seen that given a set of 3-phase average pole voltages, the difference between the maximum one and the middle-valued one is a measure of one active-state duration, and the difference between the middle-valued one and the minimum one is a measure of the other active-state
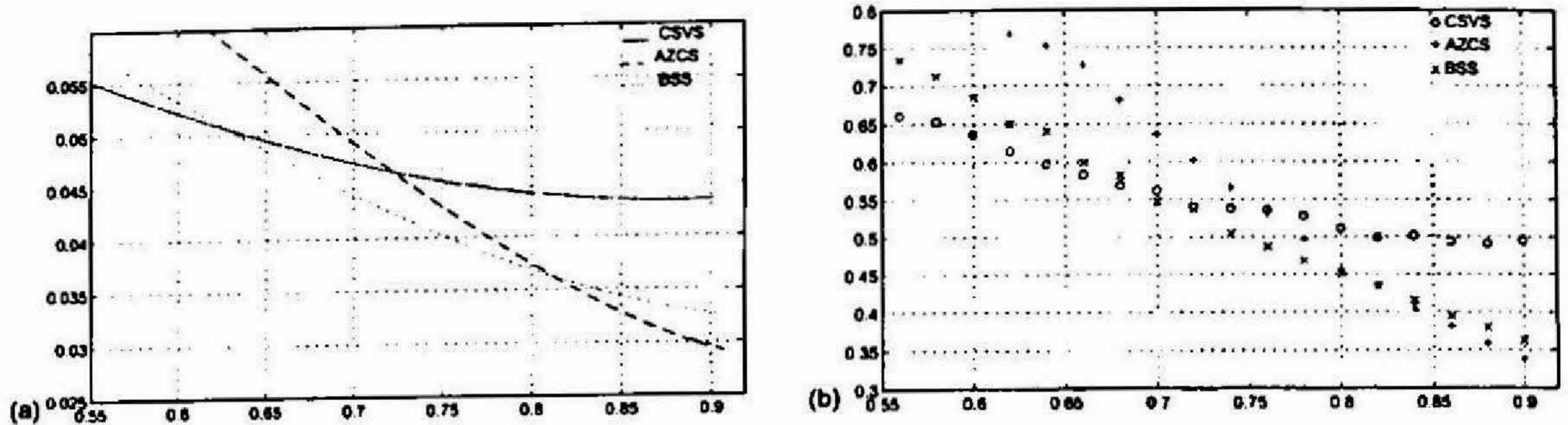
FIG. 14. Performance of different strategies for a pulse number of 9. (a) Computed V_{WTHD} vs M characteristics and (b) Measured I_{THD} vs M characteristics.

time. This is true for any set of 3-phase average pole voltages irrespective of their common-mode component. Thus, given a set of 3-phase sinusoidal modulating waves, the two active-state durations can be arrived at from them, avoiding the trigonometric calculations given in eqn (1). This has been exploited by Chung et al.[7] to simplify the calculations.

Because of this equivalence, many authors refer to the PWM techniques based both on the triangle comparison and the space vector approaches as carrier-based PWM.[5-6, 11, 12] These two are viewed as only two approaches for calculations and implementation, and are referred to as triangle intersection technique and direct digital implementation, respectively.[5-6]

However, when Type-III or IV sequences are used, the two approaches are no longer equivalent. These sequences involve the application of a state more than once within a subcycle. This means the switching of a phase more than once in the subcycle. However, switching of a phase more than once in a half-carrier cycle is not possible in the triangle comparison approach. Thus, the space vector approach is more general than the triangle comparison approach.

5. Conclusion

The division of the total zero-state duration between the two zero states is only one of the degrees of freedom available in the space vector approach. The space vector approach permits the use of different switching sequences to generate a given average vector over a subcycle. These sequences may involve the division of an active-state time, switching of a phase more than once within the subcycle, etc. Two such sequences are considered in this paper. It is shown that the PWM waveforms generated by space-vector-based techniques, using such sequences, cannot be generated by comparing suitable 3-phase modulating waves against a common triangular carrier. That is, they have no equivalence in the triangle comparison approach.

More strategies are possible with such sequences. Type-III sequences involve double switching of the phase that switches between the two active states. Sequences involving double switching of either of the other two phases can also be considered. Sequences may involve more than three switchings per subcycle also. Thus, more such sequences are possible which exploit the flexibilities in the space vector approach. As the two strategies considered help improve the performance of the drives significantly at medium and higher speed ranges, there are adequate reasons to investigate the PWM strategies using such new sequences.

References

1. SCHONUNG, A. AND STEMMLER. H.

Static frequency changers with subharmonic control in conjunction with reversible variable-speed AC drives, *Brown Boveri Rev.*, 1964, 51, 555-577.

2. VAN DER BROECK, H. W., SKUDELNY, H. C. AND STANKE, G. V.

Analysis and realisation of a pulsewidth modulator based on voltage space vectors, *IEEE Trans.*, 1988, IA-24, 142-150.

3. HANDLEY, P. G. AND BOYS, J. T.

Practical real-time PWM modulators- An assessment, *IEE Proc. B*, 1992, 139, 96-102.

4. BLASKO, V.

Analysis of a hybrid PWM based on modified space-vector and triangle-comparison methods, *IEEE Trans.*, 1997, IA-33, 756-764.

5. HAVA, A. M., KERKMAN, R. J. AND LIPO, T. A.

A high performance generalised discontinuous PWM algorithm, *IEEE Trans.*, 1998, IA-34, 1059-1071.

6. HAVA, A. M., KERKMAN, R. J. AND LIPO, T. A.

Simple analytical and graphical methods for carrier-based PWM-VSI drives, *IEEE Trans.*, 1999, PE-14, 49-61.

7. CHUNG, D. W., KIM, J. S. AND SUL, S. K.

Unified voltage modulation technique for real-time three-phase power conversion, *IEEE Trans.*, 1998, IA-34, 374-380.

8. YOUM, J-H. AND KWON, B-H.

An effective software implementation of the space-vector modulation, *IEEE Trans.*, 1999, IE-46, 866-868.

9. NARAYANAN, G. AND RANGANATHAN, V. T.

Synchronised PWM strategies based on space vector approach. Part 1: Principles of waveform generation, *IEE Proc. B*, 1999, 146, 267-275.

10. NARAYANAN, G. AND RANGANATHAN, V. T.

Synchronised PWM strategies based on space vector approach. Part 2: Performance assessment and application to V/f drives, *IEE Proc. B*, 1999, 146, 276-281.

11. HOLTZ, J.

Pulsewidth modulation - a survey, *IEEE Trans.*, 1992, IE-39, 410-420.

12. HOLTZ, J.

Pulsewidth modulation for electronic power conversion, *Proc. IEEE*, 1994, 82, 1194-1214.